# The nucleolus stress response is coupled to an ATR-Chk1–mediated G2 arrest

Hanhui Ma and Thoru Pederson
Department of Biochemistry and Molecular Pharmacology and Program in Cell and Developmental Dynamics, University of Massachusetts Medical School, Worcester, MA 01605

**ABSTRACT** **We report experiments on the connection between nucleolar stress and cell cycle progression, using HeLa cells engineered with the fluorescent ubiquitinylation-based cell cycle indicator. Nucleolar stress elicited by brief exposure of cells to a low concentration of actinomycin D that selectively inhibits rRNA synthesis had no effect on traverse of G1 or S, but stalled cells in very late interphase. Additional experiments revealed that a switch occurs during a specific temporal window during nucleolar stress and that the subsequent cell cycle arrest is not triggered simply by the stress-induced decline in the synthesis of rRNA or by a ribosome starvation phenomenon. Further experiments revealed that this nucleolus stress-induced cell cycle arrest involves the action of a G2 checkpoint mediated by the ataxia telangiectasia and Rad3-related protein (ATR)–checkpoint kinase 1 (Chk1) pathway. Based on analysis of the cell cycle stages at which this nucleolar stress effect is put into action, to become manifest later, our results demonstrate a feedforward mechanism that leads to G2 arrest and identify ATR and Chk1 as molecular agents of the requisite checkpoint.**

**Monitoring Editor**
Mark J. Solomon
Yale University

Received: Dec 13, 2012
Revised: Feb 12, 2013
Accepted: Feb 20, 2013

## INTRODUCTION

After the cytological recognition of the nucleolus in the mid-1800s, another century passed before a function of this nuclear domain was defined: the synthesis of rRNA and the assembly of nascent ribosomes (Pederson, 2011). Before that breakthrough in the mid-1960s, however, a number of cell biologists had presciently speculated that the nucleolus had something to do with progression of cells through interphase. One embodiment of this hypothesis was a study on ultraviolet light ablation of one of the two nucleoli in grasshopper neuroblasts, which resulted in a delay of progression into mitosis (Gaulden and Perry, 1958). More recently, other clues to a link between the nucleolus and the cell cycle have emerged, including the presence of growth factors in nucleoli (Pederson, 1998a), the observation of numerous cell cycle–related proteins in proteomics studies of purified nucleoli (Andersen *et al.*, 2002; Scherl *et al.*, 2002), and the discovery of nucleostemin, a nucleolus-localized protein that drives the cell cycle by attenuating the tumor suppressor p53 (Tsai and McKay, 2002; Ma and Pederson, 2008b). Although at first blush it could be imagined that these links between the nucleolus and the cell cycle might simply reflect a need for new ribosomes to advance progression through interphase, a number of considerations suggest that the situation is not that simple.

Beyond an earlier interest (Pederson, 1998a,b), we have been drawn to this issue more recently by our work with the aforementioned nucleostemin (Ma and Pederson, 2007, 2008a), and so we undertook a study in which we sought to investigate whether nucleolar homeostasis, aside from ongoing ribosome production, is related to cell cycle progression. We used an induced nucleolar stress, and our results indicate that some yet-to-be-defined normal nucleolar function (but not ribosome production) is critical for the ability of cells to progress through G2.

## RESULTS

### Nucleolar stress induces late interphase arrest

The fluorescent ubiquitinylation-based cell cycle indicator (Fucci) system was developed to visualize cell cycle progression by labeling G1-phase cells red, G1/S-transition cells yellow, and S/G2/M-phase

This article was published online ahead of print in MBoC in Press (http://www.molbiolcell.org/cgi/doi/10.1091/mbc.E12-12-0881) on February 27, 2013.

Address correspondence to: Hanhui Ma (hanhui.ma@umassmed.edu) or Thoru Pederson (thoru.pederson@umassmed.edu).

Abbreviations used: 5-EU, 5-ethynyluridine; ATR, ataxia telangiectasia and Rad3-related protein; Chk1, checkpoint kinase 1; DAPI, 4′,6-diamidino-2-phenylindole; Fucci, fluorescent ubiquitinylation-based cell cycle indicator.

© 2013 Ma and Pederson. This article is distributed by The American Society for Cell Biology under license from the author(s). Two months after publication it is available to the public under an Attribution–Noncommercial–Share Alike 3.0 Unported Creative Commons License (http://creativecommons.org/licenses/by-nc-sa/3.0).
"ASCB®," "The American Society for Cell Biology®," and "Molecular Biology of the Cell®" are registered trademarks of The American Society of Cell Biology.

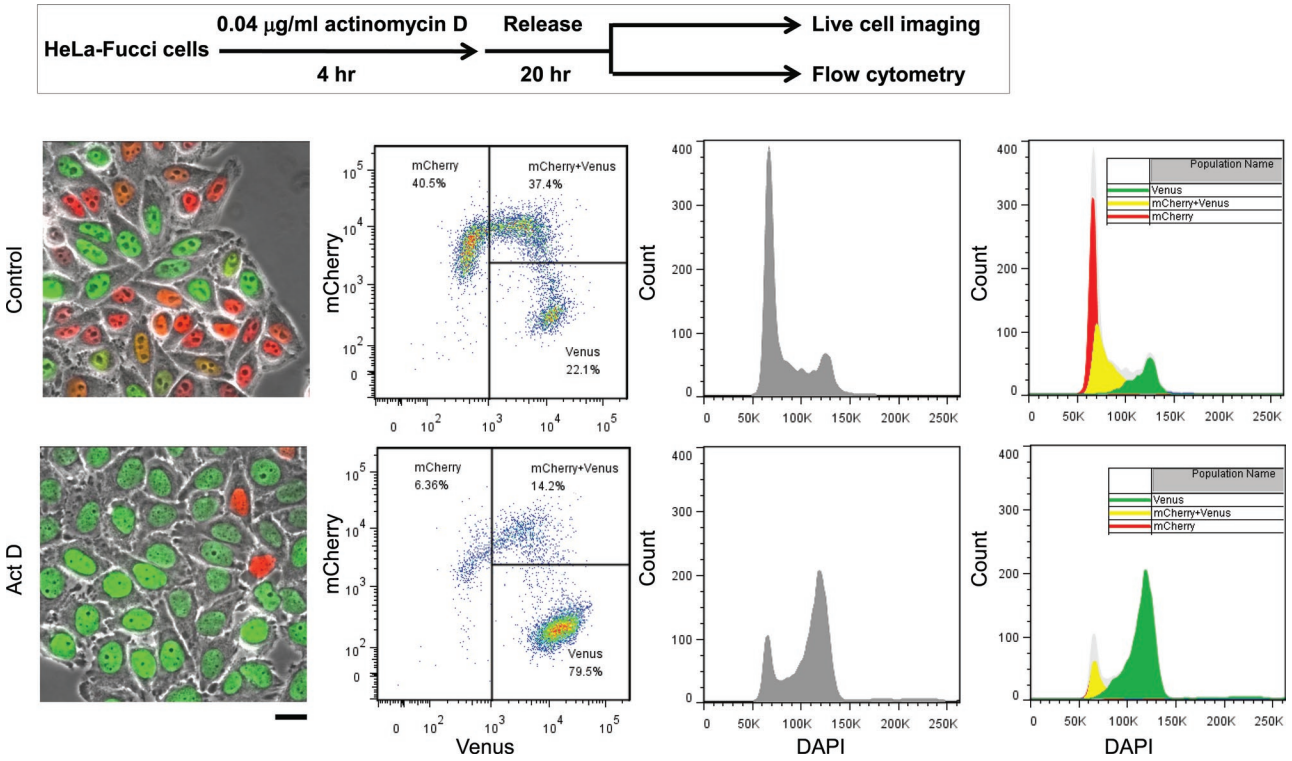


FIGURE 1: Actinomycin-induced cell cycle arrest. HeLa-Fucci cells were treated with 0.04 μg/ml actinomycin D for 4 h, and fluorescence imaging and FACS analysis were carried out after 20 h of culture in drug-free medium. Left, Representative fields showing G1 cells (red) and late S/G2/M cells (green), with occasional yellow cells; scale bar, 20 μm. Scatter plots in the next column are FACS-based intensity distributions of the two cell cycle indicator proteins tagged with mCherry and Venus (Sakaue-Sawano *et al.*, 2008), and the next two are standard DNA content profiles after DAPI staining. Rightmost are DAPI plots broken down into three distributions for each cell cycle population: mCherry (red), mCherry + Venus (yellow), and Venus (green) cells.

cells green (Sakaue-Sawano *et al.*, 2008). In the present investigation this system allowed us to precisely monitor cell cycle progression in response to nucleolar stress. Under our culture conditions, HeLa-Fucci cells displayed a G1 period of 11–12 h and a combined S-phase and G2 period of 8–9 h (Supplemental Figure S1). We treated HeLa-Fucci cells for 4 h with a concentration of actinomycin D, 0.04 μg/ml, that was previously established to selectively inhibit mammalian cell rRNA synthesis (Perry, 1962; Penman *et al.*, 1968) and induce internal repositioning of nucleolar components (Schöfer *et al.*, 1996; Dousset *et al.*, 2000). The cells were then shifted to inhibitor-free medium, and their cell cycle positions were assayed 20 h later. As shown in Figure 1 (left), cells accumulated in S, G2, and M phases during the 20 h after a 4-h treatment with actinomycin. Flow cytometry revealed that green cells constituted 79.5% of the population 20 h after actinomycin treatment, compared with a green fraction of 22.1% in untreated cells. Simultaneous flow cytometry of 4′,6-diamidino-2-phenylindole (DAPI) staining revealed that the majority of green cells had a 4C or near-4C DNA content and thus were in very late S, G2, or M. This is evident in Figure 1 (far right), where the distributions of DNA contents among red (G1), yellow (the onset of S phase), and green (S/G2/M phase) cells are overlaid.

### A switch occurs during nucleolar stress

We reasoned that if the late S/G2/M phase arrest of actinomycin-treated cells were simply a consequence of inhibiting rRNA synthesis, it should be evident after even <4 h of inhibitor treatment, since it is known that only very brief exposures are required to substantially reduce rRNA synthesis. A 25-min exposure of HeLa cells to actinomycin at 0.04 μg/ml, the concentration we used, leads to a 85% reduction in rRNA synthesis, as determined by a subsequent 10-min pulse label (Penman *et al.*, 1968). Figure 2 confirms this specifically for the HeLa-Fucci cells we used, where it can be seen that nucleolar RNA synthesis, measured by a click chemistry–based 5-ethynyluridine–labeling method (Jao and Salic, 2008), is virtually undetectable following a 30-min or 2-h exposure of cells to actinomycin (Figure 2A). However, when we looked 20 h later at RNA synthesis in cells that had been subjected to actinomycin for 30 min or 2 h, we had a surprise. As shown in Figure 2B, 20 h after a 30-min exposure to the inhibitor, nucleolar RNA synthesis had returned to the same levels as seen in untreated cells. This result was not unanticipated, as actinomycin does not bind DNA covalently, and thus a recovery of rRNA synthesis would be expected as actinomycin dissipates from the rDNA over the subsequent 20 h of culturing the cells in inhibitor-free medium. However, the striking result in Figure 2B is that in cells that were treated for 2 h, the level of nucleolar RNA synthesis 20 h later was still very depressed. Thus it is clear that at some point between a 30- and 120-min duration of nucleolar stress, a switch occurs as regards the ability of cells to resume normal rRNA synthesis levels. Yet when we looked at the steady-state level of 28S rRNA in these cells, neither the brief (30 min) nor the longer (2 or 4 h) duration of nucleolar stress had any effect on the cells' content of ribosomes (Figure 3A). This is expected because ribosomes are very stable in growing mammalian cells (e.g., Kolodny, 1975). However, as can be seen in Figure 3B, after a 30-min exposure to actinomycin, the level

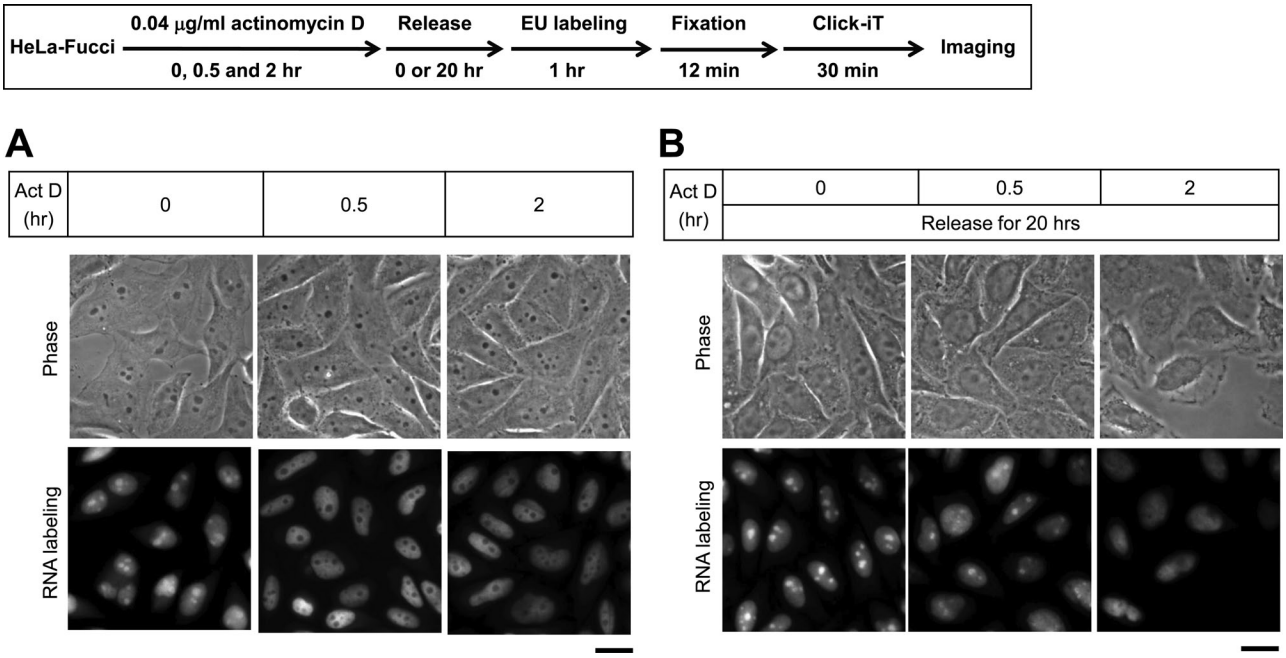


FIGURE 2: Actinomycin inhibition of nucleolar RNA synthesis. HeLa-Fucci cells treated with actinomycin for the times shown, released into inhibitor-free medium for 0 or 20 h, and then pulse labeled for 1 h with 5-EU. The levels of newly synthesized nucleolar and nucleoplasmic were detected by a click chemistry–based fluorescence tagging procedure as detailed in *Materials and Methods*. (A) RNA synthesis immediately after actinomycin treatment. (B) RNA synthesis 20 h after actinomycin treatment. Scale bar, 20 μm.

of pre-rRNA (indicative of resumed transcription of the rDNA) returned to normal levels 20 h later, whereas in cells treated with the inhibitor for 2 or 4 h, the level of pre-rRNA remained very low 20 h later. Clearly, then, there is something very different between an ~30-min and a longer actinomycin treatment, and yet none of these treatments leads to a significant negative effect of the cells' content of ribosomes (measured as total cell 28S rRNA). Furthermore, we found that protein synthesis was occurring at normal levels 20 h after a 2- or 4-h treatment with actinomycin D (Supplemental Figure S2). So, whatever the molecular basis of the cell cycle effect, it cannot be plausibly related to an impairment of translational capacity.

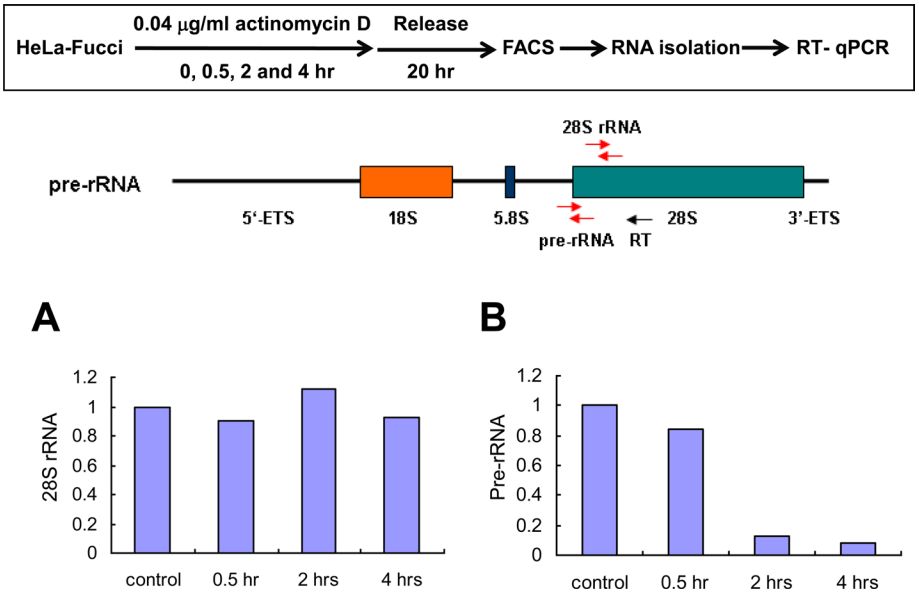


FIGURE 3: Cell cycle arrest is not due to a cell depletion of mature ribosomes. Cells were treated with actinomycin for various times (0, 0.5, 2, and 4 h) and then cultured in inhibitor-free medium for 20 h, followed by FACS selection of Venus-only cells, RNA isolation, and real-time quantitative PCR for either mature 28S rRNA (A) or pre-rRNA (B), using the primer sets indicated by the red and black arrows (see *Materials and Methods* for primer and real-time quantitative PCR details). Three replicate PCR runs were performed for each pair of primers, and the bar graphs shown are from the average values.

From these results we suspected that the situation might be more complex (and thus interesting) than initially contemplated. So we next used various durations of actinomycin treatment (0.5, 2, and 4 h), followed by culturing of cells in inhibitor-free medium for 20 h to assess cell cycle progression (Figure 4). After a 0.5-h treatment there was only a slight increase in the percentage of late S, G2, and M cells, 27.2%, as compared with 19.1% in untreated cells. Thus a brief but virtually complete inhibition of rRNA transcription 20 h earlier did not trigger a subsequent late S/G2/M-phase arrest. In contrast, when cells were treated for 2 or 4 h, the conditions of nucleolar stress from which we had established that cells cannot resume normal rRNA synthesis, 72.5 and 79.4% of the cells, respectively, became arrested (Figure 4, top; 2 and 4 h). The arrest of these cells in late S, G2, or M is further supported by the cytophotometry of DAPI-stained cells done in parallel (Figure 4, bottom; 2 and 4 h).

We next tracked individual cells to precisely observe the foregoing effects in situations in which the cell cycle position of a

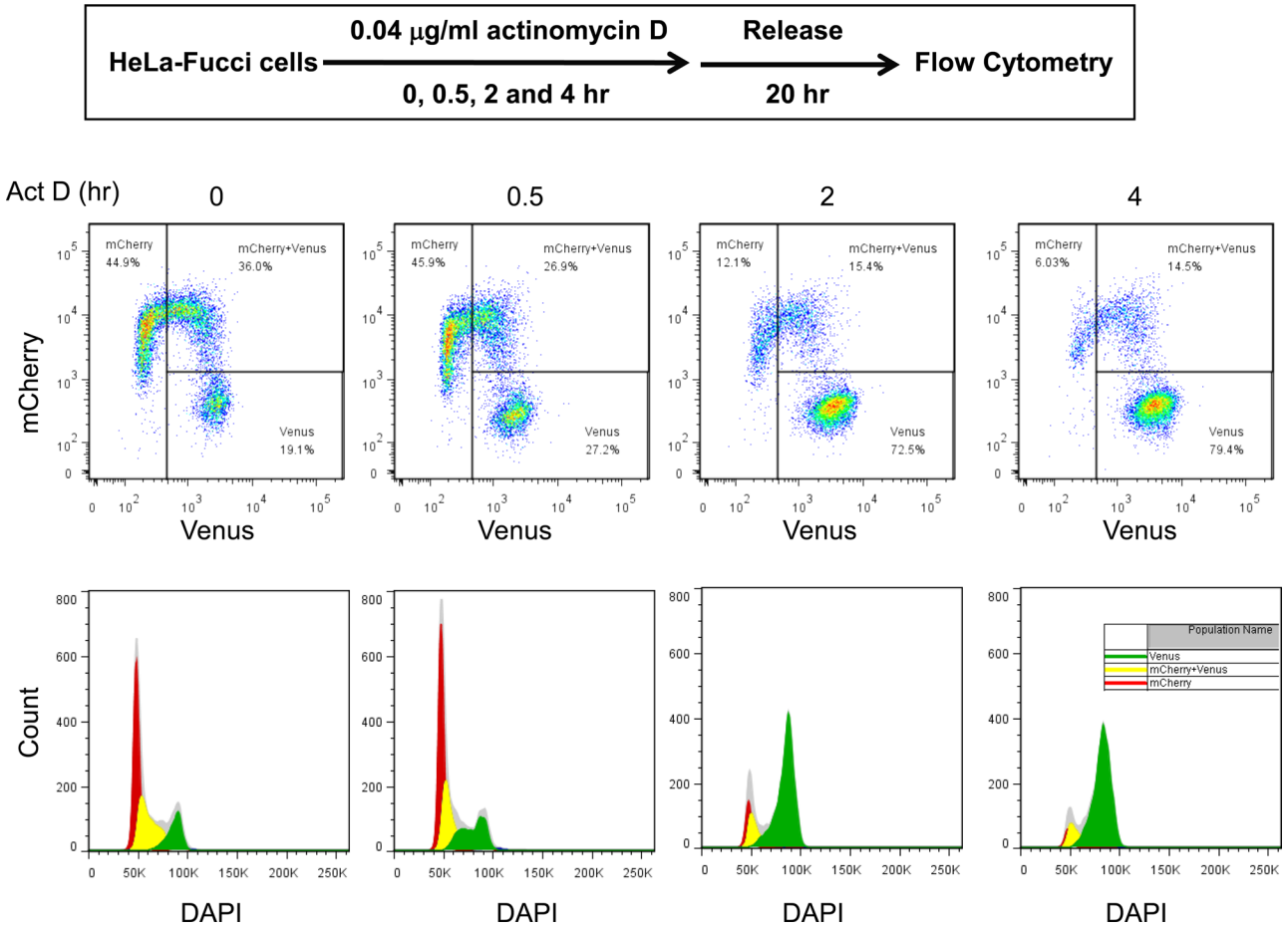


FIGURE 4: Cell cycle arrest is more pronounced after 2–4 h of nucleolar stress. Cells were exposed to actinomycin for 30 min or 2 or 4 h, and the same multicolor FACS analyses of red, yellow, green, and DAPI-stained (blue) cells were conducted as in Figure 1.

given cell at the time if treatment can be known, due to the Fucci staging colors. Figure 5A shows a series of single-cell tracking observations of cells that were in mitosis at the time of actinomycin treatment. Compared with an untreated mitotic cell (top), cells treated with actinomycin for 0.5, 2, or 4 h (the treatment commencing in mitosis in all cases) were able in all three cases to exit mitosis and progress through G1 and S with unperturbed kinetics (Figure 5A, bottom three rows), meaning that the synthesis of new ribosomes during the first 2 or 4 h of G1 (before placing the cells in inhibitor-free medium) is not required for G1 traverse and progression into S. However, the cells that were treated with actinomycin commencing at mitosis displayed a prolonged S period and G2 phase, as can be seen by that fact that even by 24 h these cells had not yet reached mitosis (Figure 5A, bottom three rows; compare with the arrival in mitosis at 20 h in the case of the untreated cell tracked in the top row). Figure 5B shows a similar set of single-cell tracking observations but in which the cells were at the onset of S phase at the time actinomycin treatment began. As shown in the top row of Figure 4B, it took 8 h for an untreated S-phase cell to reach mitosis, and from the known cell cycle parameters of these cells (Supplemental Figure S1) it can be deduced that this cell was in early S at 0 h in the tracking images. In contrast, S-phase cells treated with actinomycin for 0.5 h displayed a delay in reaching mitosis (see images with asterisk in second row of Figure 5B), but once this delayed mitosis was completed, the daughter cells progressed into G1 and into S. Moreover, the S-phase cells treated for 2 or 4 h failed to reach mitosis in even 24 h (Figure 5B, bottom two rows), in keeping with the late S/G2/M-phase arrest demonstrated in the whole population analysis (Figures 1 and 4).

### Nucleolar stress–induced cell cycle arrest involves the ataxia telangiectasia and Rad3-related protein–checkpoint kinase 1 pathway

The cell cycle arrest we observed after actinomycin treatment most plausibly involves a G2 checkpoint. Although the drug intercalates, rather than breaks, DNA, we needed to consider the possibility that a DNA-damage response was being induced. As shown in Figure 6, there was no elevation of DNA damage 20 h after a 30- or 120-min treatment with actinomycin, based on immunostaining for phosphorylated histone H2AX. In contrast, 20 h after a 120-min exposure to doxorubicin there was the expected increase in DNA damage (Fornari *et al.*, 1994). Caffeine is an inhibitor of phosphatidylinositol-3-kinase family members such as ataxia telangiectasia mutated (ATM) and ataxia telangiectasia and Rad3-related protein (ATR), which are essential for G2 checkpoint activation (Sarkaria *et al.*, 1999). As can be seen in Figure 7A (left), caffeine itself had little effect on cell cycle progression, as indicated by the similar presence of red and green cells in the two populations. As in the previous experiments, actinomycin D treatment led to an accumulation of S/G2 cells (second column, top), whereas caffeine treatment abrogated

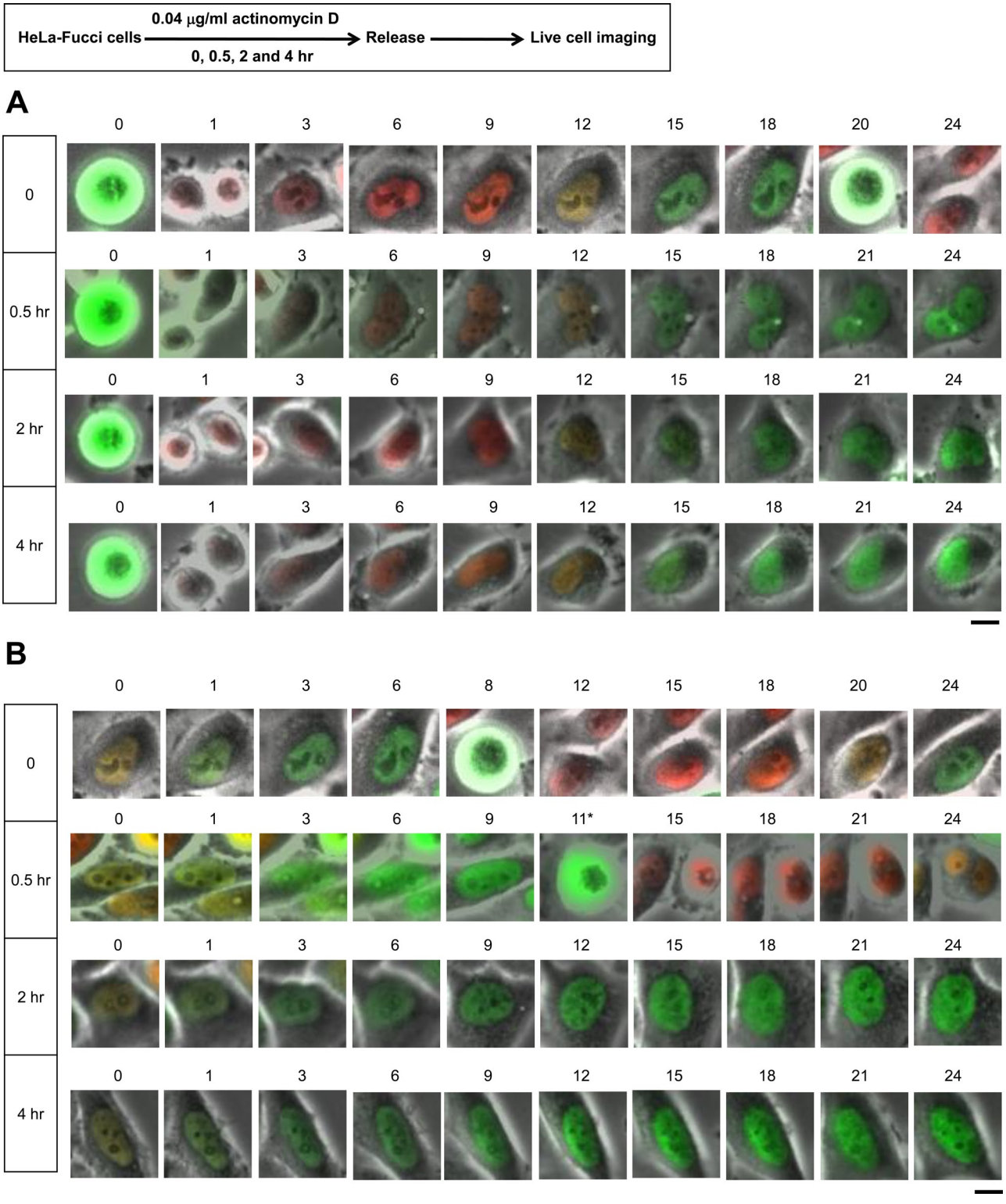


FIGURE 5: Single-cell tracking. The progression of selected cells was tracked after various times of actinomycin treatment. (A) Release of the inhibitor was at mitosis. (B) Release of inhibitor was at the G1/S transition. Scale bars, 10 μm.

this effect (second column, bottom). This result suggested that ATM and/or ATR are involved in the nucleolar stress–induced arrest, and, if so, this would define the arrest as occurring at specifically G2 as opposed to very late S or in mitosis. To further clarify this, we used UCN-01, a specific inhibitor of the ATR target checkpoint kinase 1 (Chk1; Busby *et al.*, 2000). As shown in Figure 7A (middle right column), UCN-01 had no effect on cell cycle progression in cells not subjected to nucleolar stress. However UCN-01 treatment abrogated the nucleolar stress–induced cell cycle arrest (Figure 7A, rightmost). Flow cytometry (Figure 7B) confirmed the abrogation of the

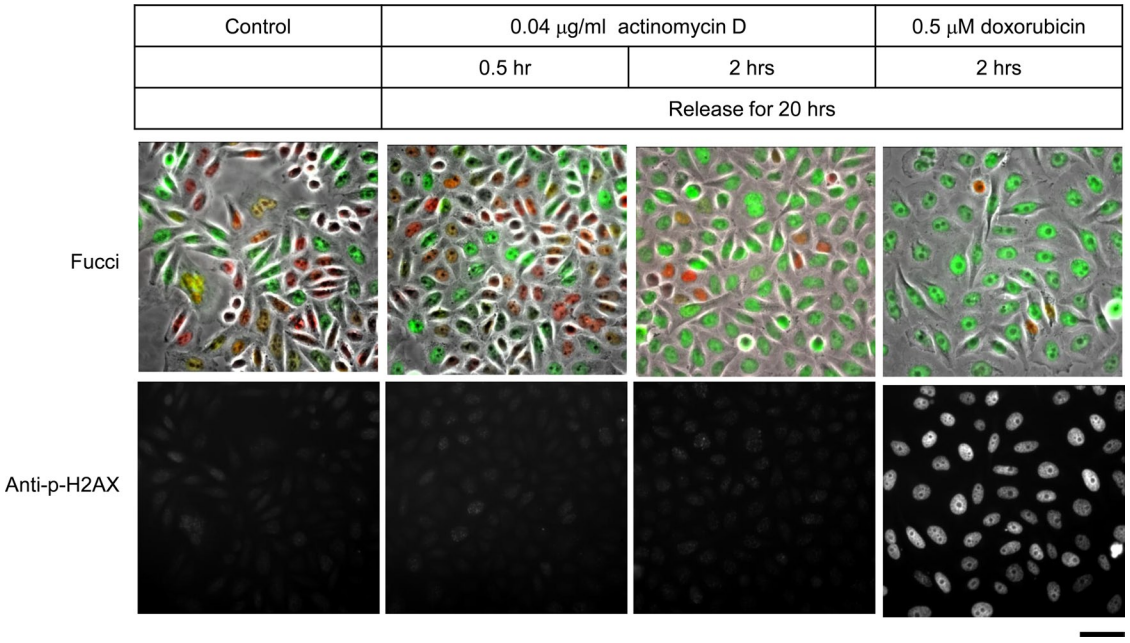


FIGURE 6: Actinomycin D treatment does not lead to DNA damage. Cells were treated with either actinomycin D or doxorubicin for the various times indicated. Phospho-H2AX was detected by immunofluorescence 20 h after treatment. Images were captured along with Fucci colors. Scale bar, 50 μm.

cell cycle arrest by caffeine. Compared to 25.5% untreated cells with a 4C DNA content, 71.4% of the actinomycin-treated cells had a 4C DNA content (bottom), compatible with the accumulation of green cells in the mCherry versus Venus fluorescence-activated cell sorting (FACS) plots (top). No appreciable effect of caffeine can be seen in both the Fucci dual-color FACS plot (top) and in the DAPI plot (bottom). In contrast, in the cells that underwent actinomycin-induced nucleolar stress in the presence of caffeine, the cell cycle distribution of cells (right) was very similar to that observed in unstressed cells both in the Fucci dual-color FACS and the DAPI plots. Figure 7C shows the results of combined nucleolar stress and caffeine or UCN-01 treatments in cells imaged at various times. The now-familiar progressive accumulation of green cells after actinomycin treatment alone (second row) contrasts with the control-like patterns observed in the caffeine- or UCN-01–treated cells. Based on the known mode of action of Chk1 (Wilsker *et al.*, 2008), its level of phosphorylation should correlate with the conditions that elicit G2 arrest. As shown in Figure 8, phosphorylation of Chk1 was elevated 20 h after a 2 h (second row, middle) or 4 h (second row, middle) actinomycin treatment, whereas no elevation was seen 20 h after a 30-min treatment (second row, middle left). Thus the results in Figures 7 and 8 define the cell cycle arrest as lying within G2 and reveal ATR and Chk1 as molecular elements in this regulatory circuit.

## DISCUSSION

The most significant step in the modern era of the nucleolus was the perception that this nuclear domain does more than build ribosomes. This idea was born in a speculative synthesis (Pederson, 1998b) but soon got traction from numerous quarters, including the discovery that the nucleolus is the site of assembly of the signal recognition particle (Jacobson and Pederson, 1998; Ciufo and Brown, 2000; Politz and Pederson, 2000; Politz *et al.*, 2000, 2002; Grosshans *et al.*, 2001; Sommerville *et al.*, 2005) and the findings that purified nucleoli harbor many proteins unrelated to ribosome biosynthesis but that have roles in cell cycle progression (Andersen *et al.*, 2002; Pederson, 2002; Scherl *et al.*, 2002). A prime example of this comes from work in budding (Shou *et al.*, 1999; Visintin *et al.*, 1999) and fission (Trautmann *et al.*, 2001) yeast showing that Cdc14 phosphatase or Cdc14-like phosphatase triggers mitotic exit by release from the nucleolus (reviewed by Amon, 2008). Increasing cases of nucleolar protein:cell cycle connections also have been seen in mammalian cells (Pederson and Tsai, 2009). The investigation reported here adds to the evidence that the nucleolus monitors cell cycle progression and that it does so outside of its role in ribosome synthesis. The notion that an interference with the non–ribosome production functions of the nucleolus could affect the cell cycle was previously raised in the context of a human disease, Diamond–Blackfan anemia. This is a neonatal-pediatric bone marrow deficiency caused by mutations in certain ribosomal proteins. A plausible case can be made that the pathogeneic trigger is an effect of these mutations on nucleolar homeostasis rather than the production of functionally impaired ribosomes per se (Pederson, 2007).

There are two caveats in this study. The G2 arrest we defined leads eventually to apoptosis (data not shown), so it is not likely to be a situation that would be tolerated in an intact organism unless the cues for apoptosis were overridden in certain cells or tissues. G2-arrested cells normally exist in many healthy mammalian tissues and are activated to enter mitosis promptly after a stimulus (Pederson and Gelfant, 1970). We of course cannot readily extrapolate the present finding with a cultured human cell line to how nucleolar stress might affect the cell cycle in an organism. The second caveat is that the mode of nucleolar stress we chose—the selective inhibition of rRNA synthesis by a low concentration of actinomycin—presumes that the rRNA genes are the only target. The selectivity of actinomycin for these genes at such low concentrations is due to their very high (~70%) G+C content and the preference of actinomycin to intercalate at G–C base pairs. However, there could be other sites in the genome with high concentrations of G–C pairs, and we cannot rule out that the observed cell cycle effects might reflect transcriptional inhibition of these putative regions.

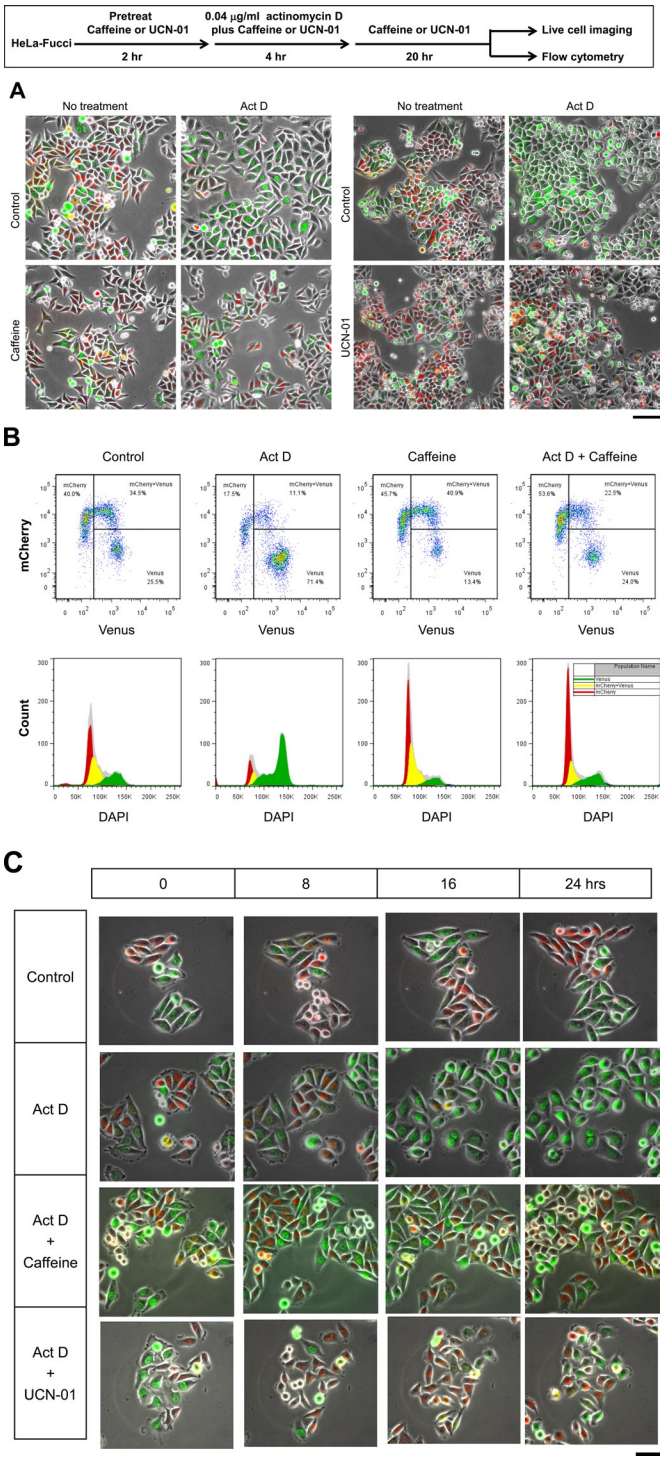


FIGURE 7: The arrest is ATR-Chk1 pathway dependent. Cells were pretreated with either caffeine or UNC-01, subjected to nucleolar stress in the presence or absence of either inhibitor, and then cultured an additional 20 h in medium lacking actinomycin but with either inhibitor. (A) Images after a 4-h nucleolar stress. Left set of four, caffeine; right set of four, UCN-01. Scale bar, 100 μm. (B) Multicolor FACS analyses of the cells shown in A. (C) Cells were exposed to ATR-Chk1 inhibitors for 2 h and then actinomycin (with continued inhibitors) for 4 h and then examined at 0, 8, 16, or 24 h. Scale bar, 50 μm.

Actinomycin D (Waksman and Woodruff, 1940), first manufactured by Merck, Sharp, and Dohme, was soon the subject of hopeful studies on tumors and cancer cell lines, yet the drug's sites of action were completely unknown. We now know, in hindsight, that the concentrations used in almost all of those early studies were ones that inhibited all three RNA polymerases. The key discovery (Perry, 1962) that a much lower concentration of the drug than had been used before selectively inhibits rRNA synthesis was a significant advance for the study of mammalian cell RNA biosynthesis. The use of low actinomycin to induce a nucleolar stress response, as in this study, has brought new insight into the control of the cell cycle. One might ponder the extent to which the rare and paradoxical successes of this drug in cancer chemotherapy (e.g., it is the front-line standard for Wilms' tumor) could have a nucleolar stress response as an underlying factor at the patient drug dosing used. Recently this notion has received some support from the development of a small-molecule inhibitor of RNA polymerase I transcription that displays a significant cytostatic selectivity for human B-cell lymphoma and leukemia cells lines relative to normal lymphocytes (Bywater *et al.*, 2012).

Although we implicated ATR-Chk1 in the G2 arrest induced by low actinomycin, it is obvious that we have not defined the entire pathway or interactome of this circuit. There may be many other players in the overall regulatory link, among which may be one or more of the many cell cycle regulatory proteins that are known to constantly shuttle between the nucleolus and extranucleolar sites in the nucleus (Pederson and Tsai, 2009; Pederson, 2011). The fact that there is a major switch in the execution of this G2 arrest pathway depending on the duration of nucleolar stress points to the existence of unknown events that occur during the stress response that, either by the schedule of their execution or by the accumulated sum of their effects, reach forward to have an effect many hours later, in G2. The study reported here thus reveals an important link between nucleolar stress and cell cycle progression but also opens many questions for future investigation.

## MATERIALS AND METHODS

### Cell culture and induction of nucleolar stress

HeLa-Fucci cells (Sakaue-Sawano *et al.*, 2008) were cultured at 37°C in DMEM (Life Technologies, Grand Island, NY) supplemented with 10% fetal bovine serum (FBS). For induction of nucleolar stress, cells were exposed to actinomycin D (Sigma-Aldrich, St. Louis, MO) for various times. In the experiments to examine the signaling pathway responsible for the induced cell cycle arrest, cells were exposed to the ATM/ATR inhibitor caffeine at 2 mM or the Chk1 inhibitor UCN-01 at 200 nM (both inhibitors purchased from Sigma-Aldrich). For single-cell tracking studies, cells were grown on Lab-Tek two-well coverglasses in 4-(2-hydroxyethyl)-1-piperazineethanesulfonic acid–buffered DMEM (21063; Life Technologies) containing 10% FBS, penicillin (100 U/ml), and streptomycin (100 μg/ml) and then overlaid with mineral oil. The microscope stage incubation chamber was maintained at 37°C as described previously (Jacobson and Pederson, 1997). Phase-contrast and fluorescence microscopy was performed with a Leica DM-IRB inverted microscope (Leica, Wetzlar, Germany) equipped a halogen lamp, a 10-position filter wheel (Sutter Instrument, Novato, CA), CFP/YFP/HcRed filter set (Semrock, Rochester, NY), a charge-coupled device camera (Photometrics, Tucson, AZ), and MetaMorph acquisition software (Molecular Devices, San Jose, CA).

### Flow cytometry

Cells were trypsinized and centrifuged at 200 g for 5 min, washed with phosphate-buffered saline (PBS), and then fixed with 4% formaldehyde in PBS for 10 min at room temperature, followed by one wash with PBS and permeabilization in 0.2% Triton X-100 in PBS for 10 min at room temperature and then another wash with PBS.

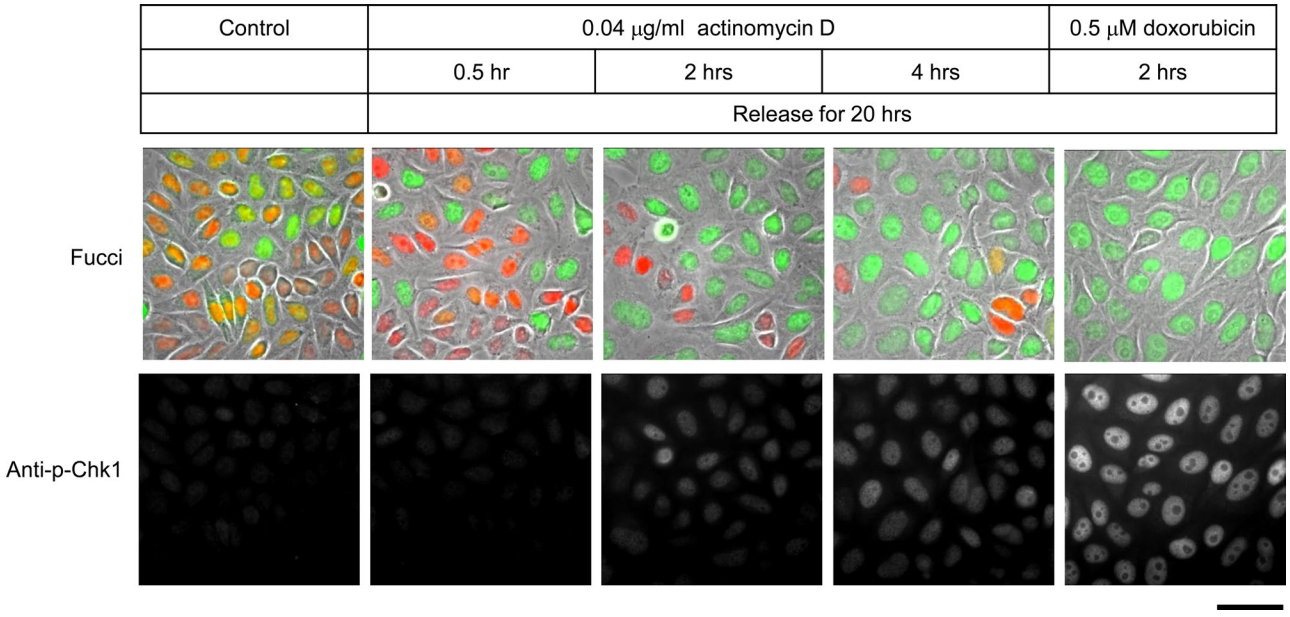


FIGURE 8: Elevation of Chk1 phosphorylation after 2–4 h of nucleolar stress. Cells were treated with either actinomycin D or doxorubicin for the various times indicated. Phospho-Chk1 was detected by immunofluorescence 20 h after treatment. Images were captured along with Fucci colors. Scale bar, 50 μm.

The cells were resuspended at $1 \times 10^6$/ml in PBS containing DAPI at 2 μg/ml (Sigma-Aldrich) and incubated for 5 min. Fluorescence-activated cell sorting was performed in the University of Massachusetts Medical School FACS Core Facility with SLR II flow cytometer (BD Biosciences, San Jose, CA) using FACSDiva software (BD Biosciences). mVenus was excited by a 488-nm laser line, and its emission was collected using a 530/30 bandpass filter; mCherry was excited by a 561-nm laser line, and its emission was collected using a 610/20 bandpass filter; Pacific blue (the violet fluorescent tag on the reaction products in the RNA synthesis assay using 5-ethynyluridine [5-EU] and click chemistry) was excited by a 405-nm laser line and its emission collected using a 450/50 bandpass filter. FACS measurements of DAPI fluorescence were done using the same 405-nm excitation and 450/50 filtered emission as for Pacific blue. FACS data were analyzed using FlowJo software (Tree Star, Ashland, OR). Sorting of cells for green fluorescence was done with a FACSAria II instrument (BD Biosciences).

### Real-time quantitative PCR

A reverse transcription primer for 28S rRNA and pre-rRNA (5′-AGTTTACCACCCGCTTTGG-3′) was combined with total cell RNA, and first-strand cDNAs were synthesized using SuperScript III reverse transcriptase (Invitrogen). The resulting cDNAs were used as templates for real-time quantitative PCR with primer sets for either 28S rRNA (forward and reverse primers 5′-AGTAACGGCGAGTGAACAGG-3′ and 5-′GCCTCGATCAGAAGGACTTG-3′, respectively) or pre-rRNA (forward and reverse primers 5′-TCTCTCTCCCGTCGCCTCT-3′ and 5′-TCTGATCTGAGGTCGCGTCT-3′, respectively), using the StepOnePlus Real-Time PCR System (Applied Biosystems, Carlsbad, CA) and the QuantiTect SYBR Green PCR kit (Qiagen, Valencia, CA).

### Imaging newly synthesized RNA or protein by click chemistry

To detect RNA synthesis, cells were treated with actinomycin for various times and then, either immediately or 20 h later, were incubated for 1 h with 5-EU at 500 μM. The cells were rinsed with PBS, fixed in 4% formaldehyde in PBS, rinsed once with PBS, and permeabilized with 0.5% Triton X-100 in PBS for 5 min. To image the sites of 5-EU incorporation, the coverslips were incubated for 30 min at room temperature in a reaction cocktail (Invitrogen) containing Pacific blue azide and the components for a copper (I)-catalyzed cycloaddition of the ethynyl groups with the azide dye (Jao and Salic, 2008). The cells were then washed twice with PBS and imaged. The images were scaled the same using MetaMorph acquisition software. For the detection of protein synthesis cells were treated with actinomycin for various times and then incubated for 1 h with L-homopropargylglycine (HPG) at 100 μM (Beatty and Tirrel, 2008). The cells were rinsed with PBS, fixed in 4% formaldehyde in PBS, rinsed once with PBS, and permeabilized with 0.2% Triton X-100 in PBS for 10 min. To image the sites of HPG incorporation, the coverslips were processed and imaged as described for detection of 5-EU incorporation.

### Immunofluorescence

Cells grown on coverslips were fixed for 12 min in PBS containing 4% formaldehyde, followed by permeabilization with 0.5% Triton X-100 for 5 min. Coverslips were then incubated with primary antibodies in PBS-1% bovine serum albumin for 1 h before washing and incubation with the Pacific blue–labeled secondary antibodies (Invitrogen). All these steps were carried out at room temperature. Coverslips were mounted in Prolong Antifade (Invitrogen) and imaged. The primary antibodies, dilutions, and suppliers were as follows: phospho–histone H2A.X (Ser-139; JBW301) mouse monoclonal antibody (1:200; Millipore, Billerica, MA) and phospho-Chk1 (Ser-317; D12H3) rabbit monoclonal antibody (1:200, Cell Signaling Technology, Beverly, MA).

## ACKNOWLEDGMENTS

We thank Pablo Reyes-Gutierrez in our lab for help with real-time quantitative PCR analyses and helpful discussions. This work was supported by grant MCB-0445841 to T.P. from the National Science Foundation.

## REFERENCES


Amon A (2008). A decade of Cdc14—a personal perspective. FEBS J 275, 5774–5778.

Andersen JS, Lyon CE, Fox AH, Leung AK, Lam YW, Steen H, Mann M, Lamond AI (2002). Directed proteomic analysis of the human nucleolus. Curr Biol 12, 1–11.

Beatty KE, Tirrell DA (2008). Two-color labeling of temporally defined protein populations in mammalian cells. Bioorg Med Chem Lett 18, 5995–5999.

Busby EC, Leistritz DF, Abraham RT, Karnitz LM, Sarkaria JN (2000). The radiosensitizing agent 7-hydroxystaurosporine (UCN-01) inhibits the DNA damage checkpoint kinase hChk1. Cancer Res 60, 2108–2112.

Bywater M *et al*. (2012). Inhibition of RNA polymerase I as a therapeutic strategy to promote cancer-specific activation of p53. Cancer Cell 22, 51–65.

Ciufo IF, Brown JD (2000). Nuclear export of yeast signal recognition particle lacking SRP54 by the Xpo1p/Crm1p NES-dependent pathway. Curr Biol 10, 1256–1264.

Dousset T, Wang C, Verheggen C, Chen D, Hernandez-Verdun D, Huang S (2000). Initiation of nucleolar assembly is independent of RNA polymerase I transcription. Mol Biol Cell 11, 2705–2717.

Fornari FA, Randolph JK, Yalowich JC, Ritke MK, Gewirtz DA (1994). Interference by doxorubicin with DNA unwinding in MCF-7 breast tumor cells. Mol Pharm 45, 649–656.

Gaulden ME, Perry RP (1958). Influence of the nucleolus on mitosis as revealed by ultraviolet microbeam irradiation. Proc Natl Acad Sci USA 44, 553–559.

Grosshans H, Deinert K, Hurt E, Simos G (2001). Biogenesis of the signal recognition particle (SRP) involves import of SRP proteins into the nucleolus, assembly with the SRP-RNA, and Xpo1p-mediated export. J Cell Biol 153, 745–762.

Jacobson MR, Pederson T (1997). RNA traffic and localization reported by fluorescent molecular cytochemistry in living cells. In: mRNA Formation and Function, ed. JD Richter, New York: Academic Press, 341–359.

Jacobson MR, Pederson T (1998). Localization of signal recognition particle RNA in the nucleolus of mammalian cells. Proc Natl Acad Sci USA 95, 7981–7986.

Jao CY, Salic A (2008). Exploring RNA transcription and turnover *in vivo* by using click chemistry. Proc Natl Acad Sci USA 105, 15779–15784.

Kolodny GM (1975). Turnover of ribosomal RNA in mouse fibroblasts (3T3) in culture. Exp Cell Res 91, 101–106.

Ma H, Pederson T (2007). Depletion of the nucleolar protein nucleostemin causes G1 cell cycle arrest via the p53 pathway. Mol Biol Cell 18, 2630–2635.

Ma H, Pederson T (2008a). Nucleophosmin is a binding partner of nucleostemin in human osteosarcoma cells. Mol Biol Cell 19, 2830–2835.

Ma H, Pederson T (2008b). Nucleostemin: a multiplex regulator of cell-cycle progression. Trends Cell Biol 18, 575–579.

Pederson T (1998a). Growth factors in the nucleolus? J Cell Biol 143, 279–281.

Pederson T (1998b). The plurifunctional nucleolus. Nucleic Acids Res 26, 3871–3876.

Pederson T (2002). Proteomics of the nucleolus: more proteins, more functions? Trends Cell Biol 27, 111–112.

Pederson T (2007). Ribosomal protein mutations in Diamond-Blackfan anemia: might they operate upstream from protein synthesis? FASEB J 21, 3442–3445.

Pederson T (2011) The nucleolus. In: The Nucleus, ed. DL Spector and T Misteli, Cold Spring Harbor, NY: Cold Spring Harbor Laboratory Press, 209–227.

Pederson T, Gelfant S (1970). G2 population cells in mouse kidney and duodenum and their behavior during the cell division cycle. Exp Cell Res 59, 32–36.

Pederson T, Tsai RY (2009). In search of non-ribosomal nucleolar protein function and regulation. Trends Cell Biol 184, 771–776.

Penman S, Vesco C, Penman M (1968). Localization and kinetics of formation of nuclear heterodisperse RNA, cytoplasmic heterodisperse RNA and polyribosome-associated messenger RNA in HeLa cells. J Mol Biol 34, 49–69.

Perry RP (1962). The cellular sites of synthesis of ribosomal RNA and 4S RNA. Proc Natl Acad Sci USA 48, 2179–2186.

Politz JC, Pederson T (2000). The nucleolus and the four ribonucleoproteins of translation. J Cell Biol 148, 1091–1095.

Politz JC, Lewandowski LB, Pederson T (2002). Signal recognition particle localization within the nucleolus differs from the classical sites of ribosome synthesis. J Cell Biol 159, 411–418.

Politz JC, Yarovoi S, Kilroy SM, Gowda K, Zwieb C, Pederson T (2000). Signal recognition particle components in the nucleolus. Proc Natl Acad Sci USA 97, 55–60.

Sakaue-Sawano A *et al*. (2008). Visualizing spatiotemporal dynamics of multicellular cell-cycle progression. Cell 132, 487–498.

Sarkaria JN, Busby EC, Tibbetts RS, Roos P, Taya Y, Karnitz LM, Abraham RT (1999). Inhibition of ATM and ATR kinase activities by the radiosensitizing agent, caffeine. Cancer Res 59, 4375–4382.

Scherl A, Couté Y, Deon C, Callé A, Kindbeiter K, Sanchez JC, Greco A, Hochstrasser D, Diaz JJ (2002). Functional proteomic analysis of human nucleolus. Mol Biol Cell 13, 4100–4109.

Schöfer C, Weipoltshammer K, Ameder Müller M, Wachtler F (1996). Redistribution of ribosomal DNA after blocking of transcription induced by actinomycin D. Chromosome Res 4, 384–391.

Shou W *et al*. (1999). Exit from mitosis is triggered by Tem1-dependent release of the protein phosphatase Cdc14 from nucleolar RENT complex. Cell 97, 233–244.

Sommerville JS, Brumwell CL, Politz JC, Pederson T (2005). Signal recognition particle assembly in relation to the function of amplified nucleoli in *Xenopus* oocytes. J Cell Sci 118, 1299–1307.

Trautmann S, Wolfe BA, Jorgensen P, Tyers M, Gould KL, McCollum D (2001). Fission yeast Clp1p phosphatase regulates G2/M transition and coordination of cytokinesis with cell cycle progression. Curr Biol 11, 931–940.

Tsai RY, McKay RD (2002). A nucleolar mechanism controlling cell proliferation in stem cells and cancer cells. Genes Dev 16, 2991–3003.

Visintin R, Hwang ES, Amon A (1999). Cfi1 prevents premature exit from mitosis by anchoring Cdc14 phosphatase in the nucleolus. Nature 398, 818–823.

Waksman SA, Woodruff HB (1940). Bacteriostatic and bacteriocidal substances produced by soil actinomycetes. Proc Soc Exp Biol 45, 609–614.

Wilsker D, Petermann E, Helleday T, Bunz F (2008). Essential function of Chk1 can be uncoupled from DNA damage checkpoint and replication control. Proc Natl Acad Sci USA 105, 20752–20757.